JMEPEG (1992) 1:801-812

Superplastic Sheet Metal Forming of a Generalized Cup Part I: Uniform Thinning

N. Chandra and D. Kannan

Superplasticity is the phenomenon observed in certain materials that deform on the order of 300 to 500% under very low flow stress, high temperature, and fine grain structure. Superplastically formed parts find application as both structural and nonstructural components in simple and complex shapes. Mathematical models that describe the forming process with optimum strain rate and tool geometry as input and pressure-time and thickness as output are essential for successful forming. This article describes the deformation of a generalized cup assuming uniform thinning in the unsupported region. Closed form equations are developed relating process parameters like pressure-time loading and thickness distribution to the shape of the cup and material properties. The generalized cup formulation is applicable to the superplastic forming of domes, right circular cylinders, deep slanted cups, and cones.

1. Introduction

SUPERPLASTICITY in materials is the ability of materials to achieve large uniform elongations only under specific conditions of temperature and strain rate.[1] Superplastic forming (SPF) is an important industrial process that has found applications in sheet metal forming in the aerospace and automotive industries. The ability to form complex shapes reduces overall manufacturing cost by reducing the total number of tool and part counts and consequently the number of forming and assembly operations. To maintain superplastic characteristics of materials under superplastic forming, forming is to be carried out at the specific optimum strain rate. Models that describe the forming process with optimum strain rate, material properties, and die geometry as input, and pressure-time and thickness-profile as output are essential not only for successful forming, but also for the overall economy of superplastic forming. Many researchers have attempted to model superplastic forming using various numerical techniques including simplified and finite-element methods. In simplified methods, the process variables are determined by assuming the shape of deformation and a specific form of thinning.[2,3] In finite-element methods, the undeformed sheet is divided into a number of continuum or structural elements depending on the planes of symmetry, and the effect of friction, material behavior, and complex geometry can be easily incorporated in these methods.[4,5] Simplified methods are attractive because they can be formulated and implemented with ease and are suitable for design situations in which the effect of variation of material property, die geometry, and sheet thickness may be studied rapidly and used as a tool for the designer to reach the final configuration.

In this article, equations describing the mechanics of deformation of a generalized axisymmetric cup are developed. The generalized cup equations can be specialized to a dome, cone, right circular cylinder, and a variety of cups with draft angles, flanges, and die entry radii by proper choice of geometric parameters. In Part I, closed form solutions are derived based on

Notations

a	Initial radius of the die opening
b	Radius of the cup when edge height is p
b_1, b_2, b_3	Constants used in volume of toroidal section in stage III
c	Radius of the cup when edge height is $p + dp$
h	Height of the pole from initial position
h_1	Height of the pole from initial to end of stage I
H	Total height of the cup
K	Material constant for superplastic material
m	Strain-rate sensitivity factor
n	Strain-hardening coefficient
P	Pressure
p	Height of the edge from initial position
ds	Infinitesimal change in thickness
dp	Infinitesimal change in edge height p
dr	Infinitesimal change in bottom radius r
dl	Infinitesimal change in slant height l
q_i	Instantaneous depth of the spherical sector
q_1	Depth of the spherical sector at the end of stage I
q_2	Depth of the spherical sector at the end of stage II
q'	Depth of the spherical sector when edge height is p
q''	Depth of the spherical sector when edge height is $p + dp$
m, c, t (subscript)	Meridian, circumference, thickness
s_0	Initial thickness
s	Current thickness
t	Time
V_{dome}	Volume of the spherical sector
V_{cone}	Volume of the material laid over the side walls
V_0	Initial volume of the superplastic sheet
V	Volume of the deformed material
V'_{dome}	Volume of the dome when edge height is p
V''_{dome}	Volume of the dome when edge height is $p + dp$
ΔV_s	Volume (incremental) laid on the side wall in stage III
ΔV_b	Volume (incremental) laid on the bottom surface in stage III
V_r	Volume of the toroid in stage III
V_{r+dr}	Volume of the toroid in stage III when radius is $r + dr$
ρ	Radius of curvature of the spherical sector
ρ_1	Radius of curvature at the end of stage I
ρ_2	Radius of curvature at the end of stage II
ρ'	Radius of curvature of the sector at p
ρ''	Radius of curvature of the sector at $p + dp$
σ	Equivalent stress
$\dot{\bar{\varepsilon}}$	Equivalent strain rate
α	Angle of inclination of the side wall

N. Chandra and **D. Kannan**, Mechanical Engineering Department, Florida A&M University, Florida State University, Tallahassee, Florida.

uniform thinning in the unsupported region, and this assumption leads to explicit relationships between various process and geometric variables. The uniform thinning assumption is strictly valid only when the material is highly superplastic (very high strain-rate sensitivity), or where the maximum final strain is not very large. In a typical forming process, there is a thickness variation in the unsupported region and, the variation has been observed experimentally by various researchers.[6-12] This is the subject of Part II. By assuming uniform thinning in the unsupported region, equations between the various process variables are developed in Part I. These equations are very useful in many preliminary investigations of superplastic forming, e.g., in establishing if a component can be formed or not, and in quickly conducting a parametric study. Such situations often arise in the design of superplastic forming components.

2. Mechanics of Dome Forming

The constitutive equation describing the mechanical behavior of superplastic material is generally given by the power-law equation $\sigma = K\dot{\varepsilon}^m$, where σ is the flow stress and $\dot{\varepsilon}$ is the strain rate. K and m are the material parameters, where K is the strength coefficient, and m is the strain-rate sensitivity factor. Other forms of equations that include the effect of grain size and strain hardening have been postulated, and an excellent review of these equations is given in Ref 1. Each superplastic material has an optimum value of $\bar{\dot{\varepsilon}}$ (or a narrow band) where maximum superplasticity is exhibited, and it is a process requirement to maintain this value of $\bar{\dot{\varepsilon}}$ at all the stages of deformation. The determination of pressure-time loading required to achieve this $\bar{\dot{\varepsilon}}$ value is the main purpose of the process model.

Certain basic assumptions are made in modeling the formation of a superplastic dome. The first stage of any axisymmetric component is a dome, as shown in Fig. 1. It is assumed that the dome is part of a spherical segment, and this geometric assumption is validated by experiments done on physical models and superplastic alloys like aluminum 7475 and Ti-6Al-4V.[6-12] However, deviation from spherical shape has also been observed when the material has low m values (less superplastic), or when the sheet is subjected to bending moments.[13] Based on experimental work performed on Zn-Al superplastic eutectoid, Brandon[13] postulated an ellipsoidal shape for the deforming dome; the parameters describing the shapes were obtained from experiments. Because the postulated shapes are arbitrary and the effects of the shape change are not significant, spherical shape with a single radius of curvature will be used in this work.

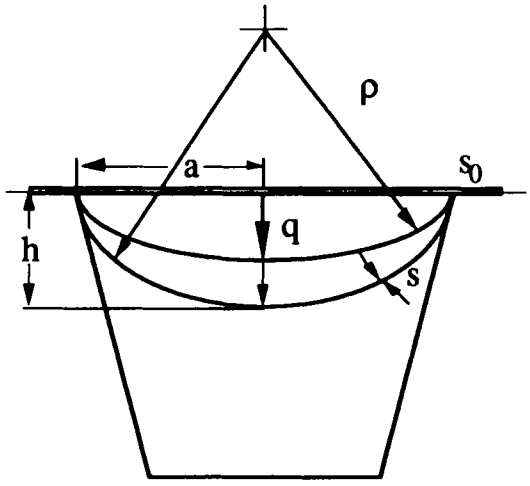

Fig. 1 Bulge forming of a superplastic sheet with geometric parameters.

For any segment whose thickness to radius of curvature ratio $s/\rho < 1/20$, the segment is considered to be a shell or else a plate, according to the membrane theory. In the case of superplastically formed component, s/ρ is normally less than this ratio, and hence, membrane theory holds good with the consequent assumption of plane stress throughout the sheet. In superplastic forming, the edge of the dome is constrained from deformation. Hence, the circumferential strain is assumed to be zero, with deformation restricted to meridian and thickness planes. The geometric center is the pole and, from symmetry considerations, is in a state of balanced biaxial stress and strain. In Part I, it is further assumed that the thickness of the sheet in the unsupported region is uniform. As will be shown in Part II, this assumption is not exact for materials with low m values, and the error increases with strain.

3. Kinematics of a Generalized Cup

In this section, the thickness at various stages of deformation of a generalized cup is described, with the assumption that the thickness is uniform in the free-forming region and that the thickness remains unchanged once the sheet contacts the die, which is the case for sticking friction.

3.1 *Dome Model*

Consider a flat superplastic circular sheet of radius a, with an initial thickness, s_0 that is allowed to form freely into a dome. The initial volume of the sheet is given by:

$$V_0 = \pi a^2 s_0 \qquad [1]$$

Figure 1 shows the free-forming dome with various geometric parameters. The radius of curvature of the deformed sheet is given by:

$$\rho = \frac{h^2 + a^2}{2h} \qquad [2]$$

where h is the instantaneous height of the dome formed (at the pole), and s is the instantaneous thickness of the deforming dome. The volume of the spherical segment is

$$V = 2\pi\rho h s \qquad [3]$$

Because the material is incompressible in the inelastic regime, the two volumes V and V_0 can be equated. Using ρ in Eq 2:

$$s = s_0\left(\frac{a^2}{h^2 + a^2}\right) \quad [4]$$

Equation 4 gives the instantaneous thickness until the sheet contacts any side wall. The thickness for hemispherical dome when $h = a$ is

$$s = \frac{s_0}{2}$$

3.2 *Generalized Cup*

Figure 2 describes the geometry of a generalized cup. The cup degenerates to a right circular cylinder when $\alpha = 0$ and to a cone when the bottom die segment shrinks to a point. The deforming surface is assumed to be part of a spherical segment with a single radius of curvature. Once the material comes in contact with the rigid die surface, it does not deform further.

The formation of a generalized cup can be divided into three stages, as shown in Fig. 2. In stage I, a circular diaphragm of superplastic material will freely deform as part of a spherical dome until it is tangent to the walls of the cup. In the second stage (stage II) of formation, the sheet metal lies over the conical surface, and the spherical sector moves down inside the die with further reduction in radius and height of the spherical sector. The third stage (stage III) of formation starts when the sheet just touches the flat bottom surface of the die. In this stage, the material is overlaid on the slanted side wall surface as well as on the bottom surface as the formation proceeds. The free-forming surface is a section of a toroidal sector, and its radius and center of curvature change with deformation.

3.2.1 *Stage I*

In stage I ($0 \le h \ge h_1$), the deformed surface of a circular sheet is assumed to be part of a sphere until it is tangent to the wall. Let h (Fig. 2) be the instantaneous height of the deformed spherical part from the initial position. In stage I, the depth of the spherical segment q is the same as the instantaneous height of deformation h.

In stage I for $0 \le h \le h_1$, s is given by Eq 4:

$$s = s_0\left(\frac{a^2}{h^2 + a^2}\right) \quad [5]$$

Because the side walls are at an angle, the maximum height of deformation, h_1, during stage I occurs when the sheet is tangent to the side walls, where:

$$h_1 = a\left(\frac{1 - \sin\alpha}{\cos\alpha}\right) \quad [6]$$

At the end of stage I, $h = h_1 = q_1$ and thickness $s = s_1$. s_1 is given by:

$$s_1 = \frac{s_0}{2}\left(\frac{\cos^2\alpha}{1 - \sin\alpha}\right) = \frac{s_0}{2}(1 + \sin\alpha) \quad [7]$$

3.2.2 *Stage II*

In the second stage of cup formation ($h_1 \le h \le H$), the pole has reached a height greater than h_1, and the side wall contact occurs. Consider the sheet that has deformed to a vertical height p along the side wall, with thickness s in the unsupported region, as shown in Fig. 3. Let the sheet deform by an infinitesimal vertical height dp with thickness $s + ds$ in the new unsupported region.

Let the radius of the spherical segment when the edge height is p be b and after a deformation of an infinitesimal vertical edge height dp be c:

$$b = a - p\tan\alpha$$
$$c = a - (p + dp)\tan\alpha \quad [8]$$

The slant height dl along the side wall is

$$dl = \frac{dp}{\cos\alpha} \quad [9]$$

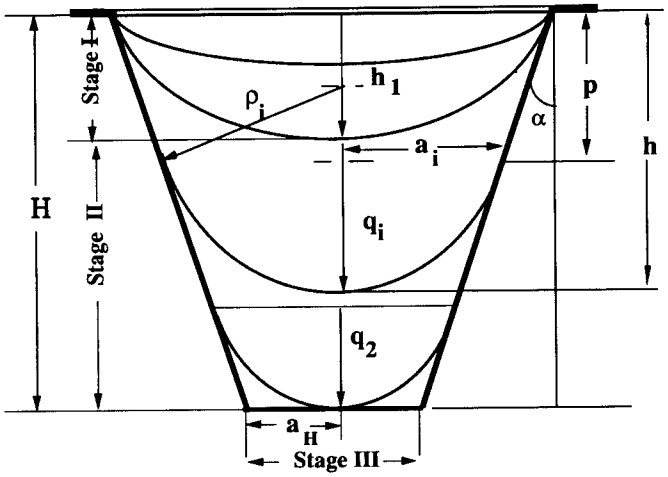

Fig. 2 Stages of deformation of a generalized cup.

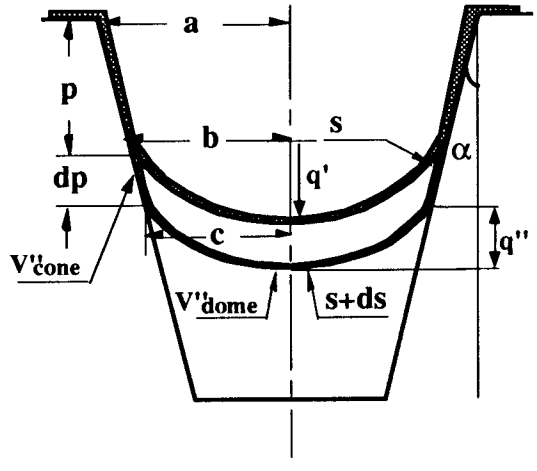

Fig. 3 Formation of deep cup during stage II.

The radius of curvature at the edge heights p and $p + dp$ be ρ' and ρ'', respectively, where:

$$\rho' = \frac{b}{\cos\alpha} = \frac{a - p\tan\alpha}{\cos\alpha}$$

and

$$\rho'' = \frac{c}{\cos\alpha} = \frac{(a - p\tan\alpha) - dp\tan\alpha}{\cos\alpha} \quad [10]$$

The depth of the spherical sectors at height p and $p + dp$ are q' and q'', respectively, as shown in Fig. 3. The volume of the unsupported spherical segment (V'_{dome}) at a height p can be expressed as a sum of the volumes of newly formed spherical segment (V''_{dome}) and truncated conical segment (V''_{dome}):

$$V'_{dome} = V''_{dome} + V''_{cone} \quad [11]$$

$$V'_{dome} = 2\pi\rho' q' s = 2\pi\rho'^2 (1 - \sin\alpha)s \quad [12]$$

Hence, the volume of the conical segment for an infinitesimal vertical height dp is

$$V''_{cone} = \pi (b + c)\, dl \left(\frac{s + s + ds}{2}\right) \quad [13]$$

$$V''_{cone} = \pi [2 (a - p\tan\alpha) - dp\tan\alpha] \frac{dp}{\cos\alpha} \left(s + \frac{ds}{2}\right) \quad [14]$$

$$V''_{cone} = 2\pi (a - p\tan\alpha) \frac{dp}{\cos\alpha} s + 2\pi (a - p\tan\alpha) \frac{dp}{\cos\alpha}\frac{ds}{2} - \pi\, dp^2 \frac{\tan\alpha}{\cos\alpha}\left(s + \frac{ds}{2}\right) \quad [15]$$

Neglecting higher order terms:

$$V''_{cone} = 2\pi (a - p\tan\alpha) \frac{dp}{\cos\alpha} s \quad [16]$$

Volume of the newly deformed spherical segment is

$$V''_{dome} = 2\pi\rho'' q'' (s + ds) \quad [17]$$

$$V''_{dome} = 2\pi\rho''^2 (1 - \sin\alpha)(s + ds) \quad [18]$$

$$V''_{dome} = 2\pi (b - dp\tan\alpha)^2 \frac{(1 - \sin\alpha)}{\cos^2\alpha} (s + ds) \quad [19]$$

$$V''_{dome} = 2\pi \frac{(1 - \sin\alpha)}{\cos^2\alpha} [b^2 (s + ds) - 2\, b\, dp\, s\tan\alpha] \quad [20]$$

Substituting the volumes in Eq 11:

$$2\pi\rho'^2 (1 - \sin\alpha)\, s = 2\pi \frac{(1 - \sin\alpha)}{\cos^2\alpha} [b^2 (s + ds) - 2\, b\, dp\, s\tan\alpha] + 2\pi (a - p\tan\alpha) \frac{dp}{\cos\alpha} s \quad [21]$$

Neglecting higher order terms:

$$2\pi b \frac{dp}{\cos\alpha} s - 2\pi \frac{(1 - \sin\alpha)}{\cos^2\alpha} 2b\, dp\, s\tan\alpha = -2\pi \frac{(1 - \sin\alpha)}{\cos^2\alpha} b^2\, ds \quad [22]$$

Rearranging and dividing the above equation by $b^2 s$:

$$\frac{ds}{s} = \frac{A}{B} \frac{dp}{(a - p\tan\alpha)} \quad [23]$$

where

$$\frac{A}{B} = \frac{\left[2\left(\frac{1 - \sin\alpha}{\cos^2\alpha}\right)\tan\alpha - \frac{1}{\cos\alpha}\right]}{\left(\frac{1 - \sin\alpha}{\cos^2\alpha}\right)} = -\left(\frac{1 - \sin\alpha}{\cos\alpha}\right) \quad [24]$$

Integrating Eq 23 with the boundary conditions given by:

$$s = s_1,\ p = 0$$
$$s = s,\ p = p \quad [25]$$

yields

$$\frac{s}{s_1} = e^{\left(\frac{1}{\sin\alpha} - 1\right)\ln\left(\frac{a - p\tan\alpha}{a}\right)} \quad [26]$$

Equation 26 gives the thickness s at any given depth p in stage II, in terms of s_1 and geometric parameters. At the end of stage II, the pole would have reached a height H, and the edge height p will be $H - q_2$, where q_2 is the depth of the spherical segment at the end of stage II. Therefore, the thickness s_2, which is s at $h = H - q_2$, is given as:

$$s_2 = \frac{s_0}{2} (1 + \sin\alpha)\, e^{\left(\frac{1}{\sin\alpha} - 1\right)\ln\left(\frac{a - (H - q_2)\tan\alpha}{a}\right)} \quad [27]$$

3.3 *Stage III*

In stage III ($0 \le r \le a_H$), the free surface assumes the shape of a toroidal sector whose radius of curvature decreases with deformation. The center of curvature moves along a line joining the center at the end of stage II and the corner of the die, as shown in Fig. 4. It can be shown that the slant height along the side wall is same as that of the bottom radius, because the deforming sheet is tangential to the die walls. Let the thickness of the toroidal section at radius r and $r + dr$ be s and $s + ds$, as shown in the Fig. 4. Let dl be the slant height of the elemental

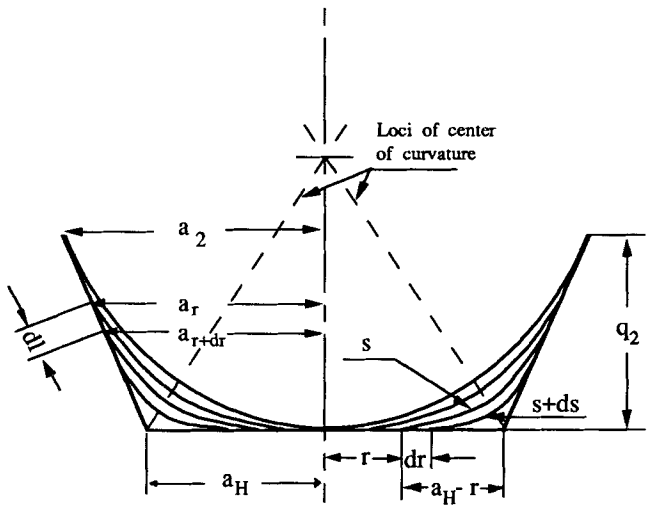

Fig. 4 Analysis of deformation in stage III.

conical surface formed while the radius at the bottom increases from r to $r + dr$. The radius of the spherical segment when the sheet has touched the bottom wall is denoted as a_2, radius of curvature as ρ_2, and depth of the spherical segment as q_2.

The centroid $\bar{x}$ of the sector formed during stage III is given by:

$$\bar{x} = \frac{r_s (1 - \sin \alpha)}{\left(\frac{\pi}{2} - \alpha\right)} \qquad [28]$$

where r_s is the radius of curvature of the sector as it deforms:

$$r_s = \rho_2 - \frac{r}{\tan \frac{\frac{\pi}{2} - \alpha}{2}}$$

The radius R about which the sector is rotated to generate the surface is $r + x$, and the surface area of the toroid is

$$V_r = 2\pi R\, l\, s = 2\pi R\, r_s \left(\frac{\pi}{2} - \alpha\right) s \qquad [29]$$

where l is the arc length of the sector. Let the volume of the conical section formed along the side walls be ΔV_s and that along the bottom wall be ΔV_b. Therefore:

$$V_r = \Delta V_s + \Delta V_b + V_{r+dr} \qquad [30]$$

where ΔV_b and ΔV_s are

$$\Delta V_b = \pi [(r + dr)^2 - r^2] (s + ds) = 2\pi r\, dr\, (s + ds) \qquad [31]$$

$$\Delta V_s = 2\pi (a_2 - r \sin \alpha)\, dr\, s + 2\pi (a_2\, dr\, ds - r \sin \alpha\, dr\, ds - r \sin \alpha\, dr\, s) \qquad [32]$$

Neglecting the higher order terms, the above two equations reduce to:

$$\Delta V_b - 2\pi r\, dr\, s$$

and

$$\Delta V_s = 2\pi (a_2 - r \sin \alpha)\, dr\, s \qquad [33]$$

The volume of the segments of the toroid formed by rotation of the sector about the axis of the cup is given, (Fig. 4) by:

$$V_r = 2\pi (b_1 + b_2 r + b_3 r^2)\, s \qquad [34]$$

and

$$V_{r+dr} = 2\pi [b_1 + b_2 (r + dr) + b_3 (r + dr)^2]\, (s + ds) \qquad [35]$$

where

$$b_1 = (1 - \sin \alpha)\, \rho_2^2 \qquad [36]$$

$$b_2 = \rho_2 \left[\left(\frac{\pi}{2} - \alpha\right) - \frac{2 (1 - \sin \alpha)}{\tan \left(\frac{\frac{\pi}{2} - \alpha}{2}\right)}\right] \qquad [37]$$

$$b_3 = \left[\frac{(1 - \sin \alpha)}{\tan^2 \left(\frac{\frac{\pi}{2} - \alpha}{2}\right)} - \frac{\left(\frac{\pi}{2} - \alpha\right)}{\tan \left(\frac{\frac{\pi}{2} - \alpha}{2}\right)}\right] \qquad [38]$$

Neglecting the higher order terms in dr and ds, the change in volume of the toroidal segment can be written as:

$$\Delta V = V_r - V_{r+dr} = -2\pi (b_1 + b_2 r + b_3 r^2)\, ds - 2\pi (b_2 + 2b_3 r)\, s\, dr \qquad [39]$$

Based on the assumption of constant volume, $\Delta V = \Delta V_s + \Delta V_b$:

$$2\pi [a_2 + r (1 - \sin \alpha)]\, s\, dr = -2\pi (b_1 + b_2 r + b_3 r^2)\, ds - 2\pi (b_2 + 2b_3 r)\, s\, dr \qquad [40]$$

which, after rearranging the terms, will yield the following relationship:

$$-\frac{ds}{s} = \frac{(a_2 + b_2) + r (1 - \sin \alpha + 2b_3)}{b_1 + b_2 r + b_3 r^2}\, dr \qquad [41]$$

If one integrates the above equation with the boundary conditions:

$$s = s_2,\ r = 0$$
$$s = s,\ r = r \qquad [42]$$

$$\ln\left(\frac{s}{s_2}\right) = -\frac{1-\sin\alpha+2b_3}{2b_3}\ln\left[\frac{b_1+b_2r+b_3r^2}{b_1}\right] + \frac{1}{y}\left[\alpha_2 - \frac{(1-\sin\alpha)\,b_2}{2b_3}\right]\ln\left[\frac{2b_3r+b_2-y}{2b_34+b_2+y}\cdot\frac{b_2+y}{b_2-y}\right] \quad [43]$$

from which one obtains the thickness $s(r)$ during stage III, where:

$$s_2 = \frac{s_0}{2}(1+\sin\alpha)\,e^{\left(\frac{1}{\sin\alpha}-1\right)\ln\left(\frac{a-(H-q_2)\tan\alpha}{a}\right)} \quad [44]$$

and

$$q_2 = [(a - H\tan\alpha)\cos\alpha] \quad [45]$$

$$y = \sqrt{b_2^2 - 4b_1b_3} \quad [46]$$

4. Special Cases of Generalized Cup

The formulations developed for the generalized cup can be specialized for specific geometry like right circular cylinder, truncated cone, and cone. The development of the formulation for these special shapes is given below and is also shown in Fig. 5.

4.1 *Right Circular Cylinder*

The generalized cup developed in the earlier section is a deep cup having a constant draft angle α to the vertical. Right circular cylinder is obtained by setting $\alpha = 0$. From Eq 4:

$$s_I = s_0\left(\frac{a^2}{h^2+a^2}\right) \quad [47]$$

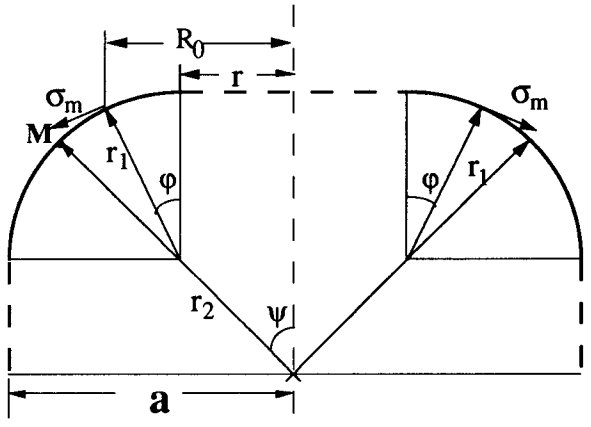

Fig. 5 Toroidal section of a cylindrical cup.

From Eq 23 for $\alpha = 0$:

$$\frac{ds}{s} = -\frac{1}{a}\left(\frac{1-\sin\alpha}{\cos\alpha}\right)dp \quad [48]$$

and upon integration yields s_{II} as:

$$s_{II} = \frac{s_0}{2}e^{-\frac{p}{a}} \quad [49]$$

where $p = h - a$. For the third stage:

$$\ln\left(\frac{s_{III}}{s_2}\right) = -\frac{1+2b_3}{2b_3}\ln\left[\frac{b_1+b_2r+b_3r^2}{b_1}\right] + \frac{1}{y}\left[a - \frac{b_2}{2b_3}\right]\ln\left[\frac{2b_3r+b_2-y}{2b_3r+b_2+y}\cdot\frac{b_2+y}{b_2-y}\right] \quad [50]$$

where s_I, s_{II}, and s_{III} are the thicknesses in respective stages, $\rho_2 = a_2$ for $\alpha = 0$ and:

$$b_1 = \rho_2^2$$
$$b_2 = \rho_2\left(\frac{\pi}{2}-2\right)$$
$$b_3 = 1 - \frac{\pi}{2} \quad [51]$$

$$s_2 = \frac{s_0}{2}e^{(1-\frac{h}{a})}$$
$$y = \sqrt{b_2^2 - 4b_1b_3} \quad [52]$$

4.2 *Truncated Cone*

The thickness profile for the truncated cone (deep slanted cup) can be determined from Eq 4, 26, and 43. For stage I:

$$s_I = s_0\left(\frac{a^2}{h^2+a^2}\right) \quad [53]$$

For stage II:

$$s_{II} = \frac{s_0}{2}(1+\sin\alpha)\,e^{\left(\frac{1}{\sin\alpha}-1\right)\ln\left(\frac{a-p\tan\alpha}{a}\right)} \quad [54]$$

and for stage III:

$$\ln\left(\frac{s_{III}}{s_2}\right) = -\frac{1-\sin\alpha+2b_3}{2b_3}\ln\left[\frac{b_1+b_2r+b_3r^2}{b_1}\right] + \frac{1}{y}\left[\alpha_2 - \frac{(1-\sin\alpha)\,b_2}{2b_3}\right]\ln\left[\frac{2b_3r+b_2-y}{2b_34+b_2+y}\cdot\frac{b_2+y}{b_2-y}\right] \quad [55]$$

from which the thickness $s(r)$ during stage III can be obtained, where constants b_1, b_2, and b_3 are given by Eq 36 to 38 and:

$$s_2 = \frac{s_0}{2}(1 + \sin\alpha)\, e^{\left(\frac{1}{\sin\alpha} - 1\right)} \ln\left(\frac{a - (H - q_2)\tan\alpha}{a}\right) \quad [56]$$

and

$$q_2 = [(a - H\tan\alpha)\cos\alpha] \quad [57]$$

$$y = \sqrt{b_2^2 - 4b_1 b_3} \quad [58]$$

4.3 *Cone*

The angle α and initial radius a determine the height H as these quantities are related by the equation $a = H \tan\alpha$. The thicknesses in stages I and II are given by Eq 4 and 26, respectively, and stage III does not exist in this case.

5. Superplastic Process Model

The kinematics of deformation developed in the previous section is used in the prediction of superplastic process parameters, which include (1) *P-t* loading profile given the optimum $\dot{\bar{\varepsilon}}$, and (2) thickness distribution in the final component.

Process modeling is a tool used to study the effect of various parameters and to determine the optimum conditions for economical forming of various shapes.[14] From the closed form solution developed for different shapes, one can determine the pressure-time cycle once the thickness profile is known. The pressure-time cycle is determined for a constant strain rate ($\dot{\bar{\varepsilon}}$) process, as explained in the following steps. In all of the cases, the height of formation is varied in discrete steps to calculate various geometric parameters using equations developed in the previous section. Once the current thickness s is known, the thickness strain ε_t is evaluated using the relation:

$$\varepsilon_t = \ln\frac{s}{s_0} \quad [59]$$

Because a state of biaxial stress is assumed, from von Mises equations, $\bar{\varepsilon} = -\varepsilon_t$ and time t is

$$t = -\varepsilon_t / \dot{\bar{\varepsilon}} \quad [60]$$

and pressure P up to the second stage of deformation is found from:

$$P = \frac{2\bar{\sigma}s}{\rho} \quad [61]$$

where $\bar{\sigma} = K\dot{\bar{\varepsilon}}^m$ is known, with the material parameters K and m known *a priori*.

In the third stage for a right circular cylinder, there are two radii of curvature for the surface of deformation; hence, the following relation is used. Let r_1 and r_2 be the two instantaneous principal radii of curvature for the toroidal section. In stage III, r_1 is the radius of curvature of the meridian plane (meridional direction), and r_2 is the radius of curvature of the parallel plane (circumferential direction). From membrane shell theories:

$$\frac{\sigma_m}{r_1} + \frac{\sigma_c}{r_2} = \frac{P}{s} \quad [62]$$

where

$$\sigma_m = \frac{P(R_0^2 - r^2)}{2\, s\, R_0 \sin\varphi} \quad \sigma_c = \frac{P(R_0 - r)}{2\, s \sin\psi} \quad [63]$$

The ratio γ is

$$\gamma = \frac{\sigma_c}{\sigma_m} = \frac{R_0}{R_0 + r\sin\psi}\frac{\sin\varphi}{} \quad [64]$$

At the middle of the sector M shown in Fig. 5, $\psi = \varphi$, and the ratio γ at that point is $(a + r)/(a + 3r)$ because $R_0 = (a + r)/2$, where a is the radius of the cylindrical cup. The meridonial stress σ_m is obtained using Eq 14:

$$\bar{\sigma} = \sigma_m \sqrt{1 - \gamma + \gamma^2} \quad [65]$$

So once γ is found, σ_m can be obtained from the above equation because effective stress is known for applying $\dot{\bar{\varepsilon}}_{opt}$ at M. The pressure P is given by Eq 63:

$$P = \frac{\sigma_m\, 2\, R_0\, s \sin\varphi}{(R_0^2 - r^{2)}} \quad [66]$$

The time of deformation from the previous step is obtained as follows. The thickness strain is $\varepsilon_t = \ln s/s_0$ and the incremental circumferential strain at M is

$$\delta\dot{\varepsilon}_c = \ln\frac{\rho_i}{\rho_{i-1}}$$

where

$$\rho_i = (a - r_i) + \frac{r_i}{\sin\pi/4}$$

and

$$\varepsilon_c = \varepsilon_c \text{ at } (i-1) + \delta\varepsilon_c$$

and $\varepsilon_m = -(\varepsilon_t + \varepsilon_c)$. The equivalent strain is given by:

$$\bar{\varepsilon} = \left[\frac{4}{3}(\varepsilon_m^2 + \varepsilon_c^2 - \varepsilon_m\varepsilon_c)\right]^{\frac{1}{2}} \quad [67]$$

From effective strain $\bar{\varepsilon}$, the total time of formation t is evaluated as:

$$t = \frac{\bar{\varepsilon}}{\dot{\bar{\varepsilon}}} \quad [68]$$

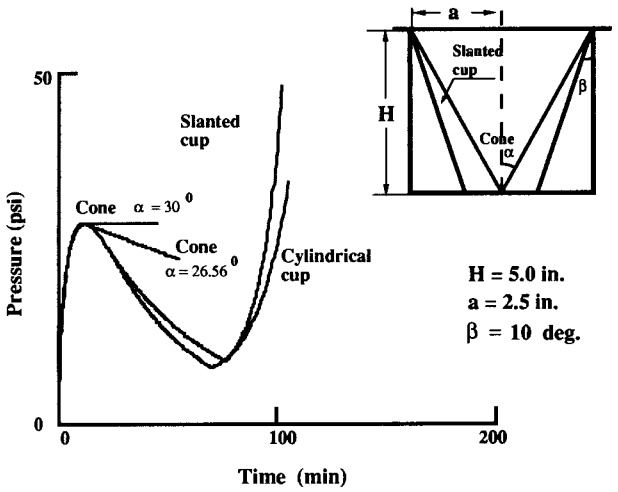

Fig. 6 Pressure-time cycle for cone, deep slanted, and cylindrical cups.

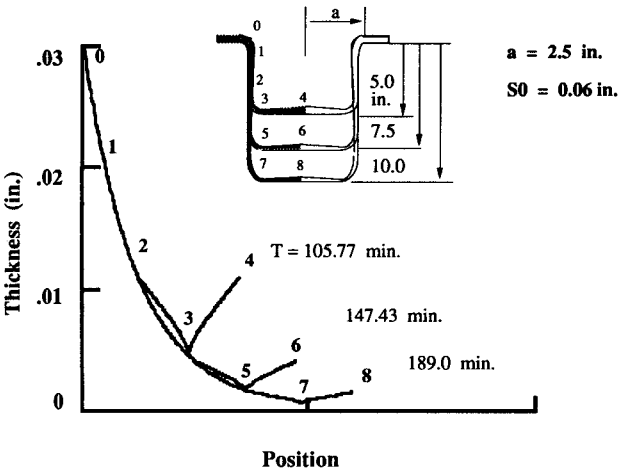

Fig. 7 Thickness profile for cylindrical cups of various heights (aluminum 7475).

6. Results and Discussion

Equations developed in the previous sections were used in the solution to superplastic forming problems of right circular cylinders, deep slanted cups, and cones. Pressure-time loading to maintain optimum $\bar{\dot{\varepsilon}}$ was determined by successively solving the equations for increasing depth in stages I and II and radius in stage III. Thickness s at various instants of time t can also be calculated, which yield the final formed thickness distribution in the component.

The computer program was written in FORTRAN 77 and was executed on a VAX 2000 workstation with VMS operating system. The program is capable of handling different shapes by appropriate choice of draft angle α and bottom width a_H, as shown in Fig. 6. Because the model is statically determinate, the thickness profile is insensitive to material parameters; however, pressure-time depends on the form of the constitutive equations and the actual value of the material constants.

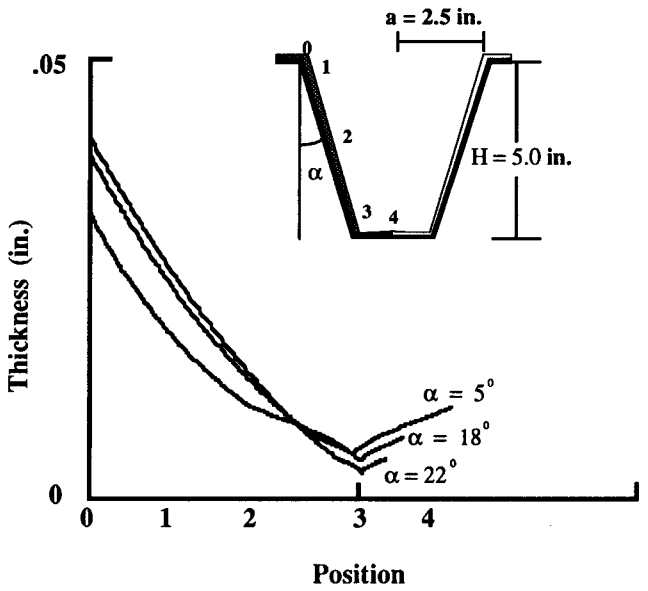

Fig. 8 Thickness profile for slanted cups of different angle α (aluminum 7475).

Figure 6 shows the pressure-time profile for a cone, slanted cup, and a cylindrical cup. The dimensions are shown in Fig. 6 also. The plot is identical for all of these shapes up to the initial peak pressure, and then there is a linear drop in pressure in the case of cone because s/ρ varies linearly. A cone angle of $\alpha = 30°$ maintains a constant $\bar{\dot{\varepsilon}}$ by the application of uniform pressure in stage II, as shown in the Appendix. This appendix also shows that, with the assumption of uniform thinning, it is not necessary to design a variable cone angle for the mechanical characterization test using uniform pressure. This result differs from that shown in a technical report by McDonnell Douglas Corp.[15,16] In the case of cylindrical and slanted cups, there is a decrease in pressure in stage II and a rapid increase in pressure in stage III. In the case of a cylindrical cup, ρ remains constant in stage II, and the rate of decrease of ρ is less severe in stage III compared to a slanted cup. This is reflected in the rapid increase in pressure in stage III for a slanted cup. Also, for same total height of the cylindrical and slanted cup, the pressure during stage II remains very close because the ratio s/ρ for a 10° slanted cup is approximately the same as that of the other. However, for a cone of the same total height, s/ρ is higher, leading to a higher pressure.

Figures 7 to 9 show the final thickness distribution of the cylindrical cups, slanted cups, and cones for various geometric and material parameters. The results of forming given in these plots follow the power-law model $\bar{\sigma} = K\,\bar{\dot{\varepsilon}}^m$, where the material constants $K = 67500$ lbf/(in.^{2} sec^m) and $m = 0.55$ for aluminum 7475 alloy and the optimum strain rate is $\bar{\dot{\varepsilon}} = 0.0004$/s. Figure 7 shows the thickness distribution for cylindrical cups of different heights and the same radii. The thickness distribution along the side wall follows the same curve until it contacts the bottom surface of the respective cups. The thickness at the center of the bottom wall is higher than the corners. Minimum thickness oc-

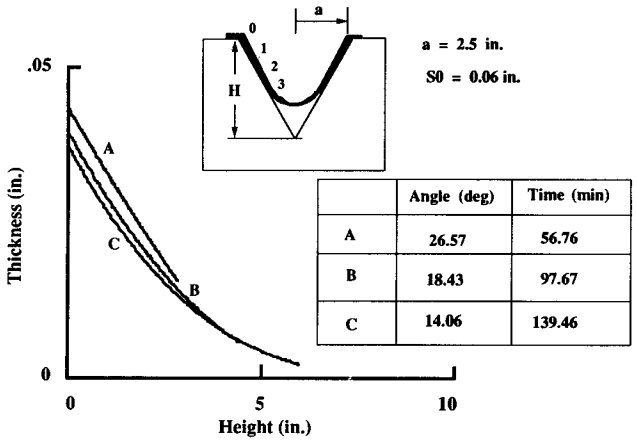

	Angle (deg)	Time (min)
A	26.57	56.76
B	18.43	97.67
C	14.06	139.46

Fig. 9 Thickness profile for cones of various half cone angles (aluminum 7475).

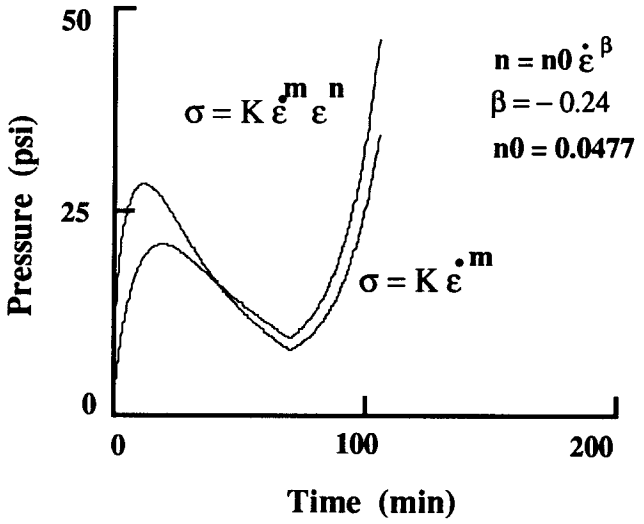

Fig. 10 Effect of strain hardening on forming cycle for an aluminum 7475 alloy for a cylindrical cup.

curs in the bottom corner where the sheet forms last, because the sheet, after bottom contact, does not deform under sticking conditions. It is also clear from the plot that the variation in thinning is not linear over the side and bottom walls, as shown in the equations for the spherical and toroidal sections.

Figure 8 shows the thickness distribution for slanted cups of different draft angle α. It can be observed from the thickness profiles that the higher the slope of the side wall, the higher the side wall thickness at the top edge. Because the thickness along the side wall is less in lower slopes, more volume is available for formation of stage III, resulting in a higher thickness profile and causing a crossover, as shown in Fig. 8. The thickness along the side wall is plotted against the vertical height of the points along the surface. The position numbers refer to the locations at the same vertical height along the side wall. The minimum thickness occurs at the corners, which refers to position 3 on the plot.

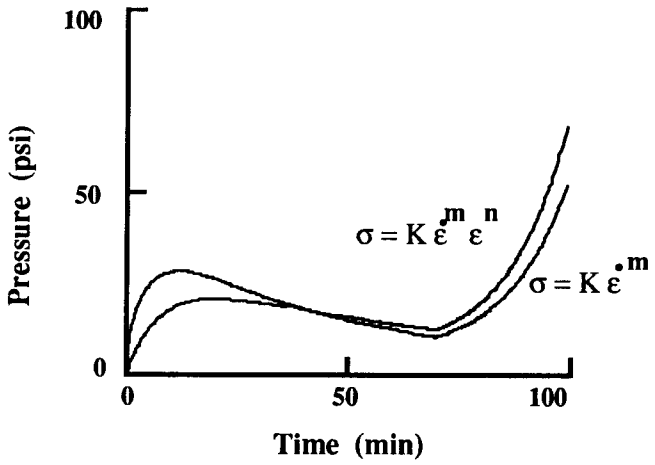

Fig. 11 Effect of strain hardening on forming cycle for a cup of 10° slant angle (aluminum 7475).

Figure 9 shows the thickness distribution for cones of different half cone angle α. The angle, total height of the cone, and time of formation are given in tabular form. The entry die radius a being the same, the total height H is increased to obtain smaller half cone angle. The thickness profile is higher for a higher half cone angle. In the case of a cone, there is no stage III formation in a generalized cup. The above thickness profiles are plotted with the height of formation equal to 80% of the height of stage II. The crossover in thickness profile can be observed as the cone reaches very close to the bottom, which was also observed in the deep slanted cup.

Figure 10 shows the effect of different forms of constitutive equations on the formability of superplastic alloy. Based on experimental data, Story *et al.*[17] suggested a strain-hardening model $\sigma = K \dot{\varepsilon}^m \varepsilon^n$, were n is the strain-hardening index, which is expressed as $n = n_0 \dot{\varepsilon}^{\beta}$. For aluminum 7475 alloy, the constants are determined by superplastic uniaxial tension testing[17] as $n_0 = 0.0477$ and $\beta = -0.24$. In the strain-hardening model, the forming pressure is less in stage I compared to the power-law model $\sigma = K\dot{\varepsilon}^m$ because the stress is low in the initial stages, but increases from the middle of stage II where the strain is relatively higher. In Fig. 11, the same effects of strain hardening are shown for a deep slanted cup of 10° draft angle. Similar trends are observed for slanted cup as in the previous case. It should be noted that there is no variation in final thickness distribution as already stated.

7. Summary and Conclusion

Thickness profile in a generalized cup is evaluated based on the geometry of the forming profile. The equations are also applicable to cone, right circular cylinder, and deep slanted cups. Uniform thinning distribution is assumed in the unsupported region, and the thickness of the sheet is assumed to remain constant once in contact with the die. Pressure-time relationships are developed for maintaining superplastic conditions in the deforming materials, and the final thickness of components for these shapes is determined.

8. Acknowledgement

The authors wish to acknowledge the National Science Foundation and General Dynamics Corporation for their financial support during the course of this research.

References

1. K.A. Padmanabhan and G.J. Davis, *Superplasticity*, Springer-Verlag, 1953
2. N. Chandra and R.E. Goforth, "An Analytical Model for Axisymmetric Superplastic Metal Forming Process," TMS Technical Paper No. A 87-11, The Metallurgical Society, 1987
3. N. Chandra and B. Roy, Membrane Element Analysis of Axisymmetric and Nonaxisymmetric Superplastic Metal Forming Processes, in *Superplasticity and Superplastic Forming*, C.H. Hamilton and N.E. Paton, Ed., TMS Publishers, 1988, p 283
4. J. Bonet and R.D. Wood, Solution Procedures for the Finite Element Analysis of Superplastic Forming of Thin Sheet, *Proc. Int. Conf. Computational Plasticity Models, Software and Applications*, Part 2, Pineridge Press, 1987, p 927
5. N. Chandra, Analysis of Superplastic Metal Forming by a Finite Element Method, *Int. J. Num. Method. Eng.*, Vol 26, 1988, p 1925
6. D.L. Holt, Analysis of the Bulging of a Superplastic Sheet by Lateral Pressure, *Int. J. Mechan. Sci*, Vol 12, 1970, p 491
7. F. Jovane, An Approximate Analysis of the Superplastic Forming of a Thin Circular Diaphragm: Theory and Experiments, *Int. J. Mechan. Sci.*, Vol 10, 1968, p 403
8. G.C. Cornfield and R.H. Johnson, The Forming of Superplastic Sheet Metal, *Int. J. Mechan. Sci.*, Vol 12, 1970, p 479
9. D. Viswanathan, S. Venkataswamy, and K.A. Padmanabhan, Theoretical and Experimental Studies on the Pressure Thermoforming of Hemispheres of Alloy Ti-6Al-4V, in *Superplasticity and Superplastic Forming*, The Metallurgical Society, 1988, p 321
10. S.T.S. Al-Hassani, G.G.W. Clemas, and T.Y.M. Al-Naib, The Free Bulge Forming of Zn-Al Superplastic Sheet from a Circular Die, *Proc. 18th Int. Machine Tool Design and Research Conf.*, J.M. Alexander, Ed., London, 1977, p 361
11. D.-J. Zhou and J. Lian, Numerical Analysis of Superplastic Bulging for Cavity-Sensitive Materials, *Int. J. Mechan. Sci*, Vol 29, 1987, p 565
12. A.K. Ghosh and C.H. Hamilton, Superplastic Forming of a Long Rectangular Box Section Analysis and Experiment, *Proc. ASM Process Modeling Fundamentals and Applications to Metals*, ASM, 1978, p 303
13. J.F. Brandon, H. Lecoanet, and C. Oytana, A New Formulation for the Bulging of Viscous Sheet Metals, *Int. J. Mechan. Sci.*, Vol 21, 1979, p 379
14. N. Chandra, "Process Modeling of SPF Processes," SME Technical Paper No. MR89-473, Society of Manufacturing Engineers, 1989
15. T.L. Mackay, S.M.L. Sastry, and C.F. Yolton, "Mechanical Characterization of Superplastic Materials using Variable Modified Cone Test," Douglas-Aircraft Co., McDonnell Douglas Corp., Technical Report AFWAL-TR-80-4038, 1980
16. R.E. Goforth, N. Chandra, and D. George, Mechanical Characterization of Superplastic Material using Variable Modified Cone Test, in *Superplasticity in Aerospace*, H.C. Heikkenen and T.R. McNelley, Ed., The Metallurgical Society, 1988, p 149
17. J.M. Story, J.I. Petit, D.J. Lege, and B.L. Hazard, The Effect of Forming Process Variables on Cavitation in the Superplastic Forming of 7475 Aluminum, *Proc. Int. Conf. Superplasticity in Aerospace-Aluminium*, Cranfield, England, 1985, p 67

Appendix

Consider a cone of die radius a, initial thickness s_0, and half cone angle α, as shown in Fig. A1(a). The thickness s_1 at the end of stage I is given by Eq 7 as:

$$s_1 = \frac{s_0}{2}(1 + \sin\alpha) \qquad [A1]$$

radius of curvature ρ_p is given by Eq 10 as $\rho_p = (a - p\tan\alpha)/\cos\alpha$, and thickness at a height p from the initial position is given by Eq 26 as:

$$s_p = s_1 e^{\frac{1-\sin\alpha}{\sin\alpha}\ln\frac{a-p\tan\alpha}{a}} \qquad [A2]$$

For constant pressure during the second stage of cone forming, the following relationship needs to be satisfied, where ρ_1 is the radius of curvature at the end of stage I:

$$\frac{\rho_1}{s_1} = \frac{\rho_p}{s_p} \qquad [A3]$$

Now substituting the actual values in the above relation yields:

$$\frac{\frac{a}{\cos\alpha}}{s_1} = \frac{\frac{a-p\tan\alpha}{\cos\alpha}}{s_1 e^{\frac{1-\sin\alpha}{\sin\alpha}\ln\frac{a-p\tan\alpha}{a}}} \qquad [A4]$$

By simplifying and rearranging the terms:

$$\frac{a-p\tan\alpha}{a} = e^{\frac{1-\sin\alpha}{\sin\alpha}\ln\frac{a-p\tan\alpha}{a}} \qquad [A5]$$

Raising the above equation to logarithm on both sides:

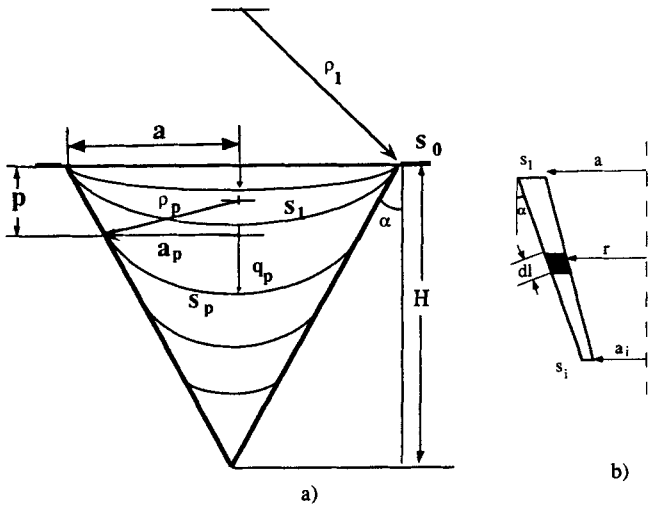

Fig. A1 **(a)** Geometry of deformation in a constant angle cone. **(b)** Truncated cone with varying wall thickness.